the series of long range H-H coupling constants was encountered by Anet et al.[36] In a series of half-cage molecules with oxygen atoms both inside and outside, it was found that coupling was exceedingly small for protons separated by six to seven bonds. However, it was concluded[36] that interaction *through* an oxygen atom in one of the compounds led to appreciable coupling.

Acknowledgment. The authors wish to thank Professor J. B. Grutzner for obtaining some of the ^{13}C NMR spectra and the University of Arizona Computer Center for computational facilities.

References and Notes

(1) (a) University of Arizona; (b) The University of New England; (c) School of Science, Griffith University, Nathan, Brisbane, Queensland. Queen Elizabeth II Research Fellow, 1973–1974.
(2) M. Karplus, *J. Chem. Phys.*, **30**, 11 (1959); M. Karplus, *J. Am. Chem. Soc.*, **85**, 2870 (1963).
(3) M. Barfield and D. M. Grant, *Adv. Magn. Reson.*, **1**, 149 (1965); A. A. Bothner-By, *ibid.*, 1, 195 (1965).
(4) M. Barfield and H. L. Gearhart, *J. Am. Chem. Soc.*, **95**, 641 (1973).
(5) J. H. Marshall and D. E. Miller, *J. Am. Chem. Soc.*, **95**, 8305 (1973). References to a number of types of vicinal coupling are included in the references to this paper.
(6) S. Karplus and M. Karplus, *Proc. Natl. Acad. Sci. U.S.*, **69**, 3204 (1972); R. Wasylishen and T. Schaefer, *Can. J. Chem.*, **50**, 2989 (1972); M. Barfield and H. L. Gearhart, *Mol. Phys.*, **27**, 899 (1974).
(7) D. Doddrell, I. Burfitt, W. Kitching, M. Bullpitt, C. Lee, R. J. Mynott, J. L. Considine, H. G. Kuivila, and R. H. Sarma, *J. Am. Chem. Soc.*, **96**, 1640 (1974).
(8) M. Barfield and M. Karplus, *J. Am. Chem. Soc.*, **91**, 1 (1969).
(9) A. I. Vogel, "Practical Organic Chemistry", Longmans, London, 1956.
(10) R. R. Sauers, *J. Am. Chem. Soc.*, **81**, 4873 (1959).
(11) H. H. Zeiss and D. A. Pease, Jr., *J. Am. Chem. Soc.*, **78**, 3182 (1956).
(12) E. Wenkert, A. O. Clouse, D. W. Cochran, and D. Doddrell, *J. Am. Chem. Soc.*, **91**, 6879 (1969).
(13) H. J. Reich, M. Jautelat, M. T. Messe, F. J. Weigert, and J. D. Roberts., *J. Am. Chem. Soc.*, **91**, 7445 (1969).
(14) J. B. Stothers, "Carbon-13 NMR Spectroscopy", Academic Press, New York, N.Y., 1972.
(15) P. S. Pregosin and E. W. Randall in "Determination of Organic Structures by Physical Methods", F. C. Nachod and J. J. Zuckerman, Eds., Academic Press, New York, N.Y., 1971.
(16) J. A. Pople, J. W. McIver, Jr., and N. S. Ostlund, *J. Chem. Phys.*, **49**, 2960, 2965 (1968).
(17) J. A. Pople, D. L. Beveridge, and P. A. Dobosh, *J. Chem. Phys.*, **47**, 2026 (1967).
(18) P. A. Dobosh, Program No. 142 (modified by M. Barfield and M. D. Johnston, Jr.), Quantum Chemistry Program Exchange, University of Indiana, Bloomington, Indiana.
(19) J. A. Pople and M. Gordon, *J. Am. Chem. Soc.*, **89**, 4253 (1967).
(20) L. E. Sutton, Ed., *Chem., Soc., Spec. Publ.*, **No.** 11 (1958); **No.** 18 (1965).
(21) R. M. Lynden-Bell and N. Sheppard, *Proc. R. Soc. London, Ser. A*, **269**, 385 (1962); D. M. Graham and C. E. Holloway, *Can. J. Chem.*, 41, 2114 (1963).
(22) K. D. Summerhays and G. E. Maciel, *J. Am. Chem. Soc.*, **94**, 8348 (1972).
(23) F. J. Weigert and J. D. Roberts, *J. Am. Chem. Soc.*, **94**, 6021 (1972).
(24) K. Frei and H. J. Bernstein, *J. Chem. Phys.*, **38**, 1216 (1963).
(25) N. Muller and D. E. Pritchard, *J. Chem. Phys.*, **31**, 768 (1959).
(26) M. Barfield, *J. Chem. Phys.*, **44**, 1836 (1966).
(27) A. C. Blizzard and D. P. Santry, *J. Chem. Phys.*, **55**, 950 (1971).
(28) J. M. Schulman and M. D. Newton, *J. Am. Chem. Soc.*, **96**, 6295 (1974).
(29) D. Doddrell, I. Burfitt, J. B. Grutzner, and M. Barfield, *J. Am. Chem. Soc.*, **96**, 1241 (1974).
(30) Because of an error in the conformational data for butanoic acid the coupling constant values reported for some of the nonplanar conformations of butanoic acid were in error in ref 29. The corrected values are given in Table III.
(31) K. L. Servis and K. N. Fang, *J. Am. Chem. Soc.*, **90**, 6712 (1968).
(32) G. W. Gribble and J. R. Douglas, Jr., *J. Am. Chem. Soc.*, **92**, 5764 (1970)
(33) K. Hirao, H. Nakatsuji, and H. Kato, *J. Am. Chem. Soc.*, **95**, 31 (1973).
(34) R. Wasylishen and M. Barfield, *J. Am. Chem. Soc.*, submitted for publication.
(35) M. Barfield, A. M. Dean, C. J. Fallick, R. J. Spear, S. Sternhell, and P. W. Westerman, *J. Am. Chem. Soc.*, **97**, 1482 (1975).
(36) F. A. L. Anet, J. R. Bourn, P. Carter, and S. Winstein, *J. Am. Chem. Soc.*, **87**, 5249 (1965).

Ab Initio SCF–MO Calculations on Carbanions. Methyl, Ethyl, Vinyl, and Ethynyl Anions[1]

James E. Williams, Jr., and Andrew Streitwieser, Jr.*

Contribution from the Department of Chemistry, University of California, Berkeley, California 94720. *Received August 24, 1974*

Abstract: The results of SCF–LCAO–MO calculations on methyl, ethyl, vinyl, and ethynyl anions are presented and compared with the parent hydrocarbons. The basis sets used include the minimum basis set, STO-4G, and extended basis sets of split shell (SS), including for some cases additional polarization functions, d on carbon (SS+d) and p on hydrogen (SS+d,p). Electron density and electron density difference functions are presented as three-dimensional perspective plots and are used to evaluate the electronic changes that occur on ionization of a C–H bond. Other energy quantities such as electron affinities and proton affinities are presented and discussed in addition to geometries and inversion barriers.

Carbanions are among the important intermediates in organic chemistry but their study presents a number of problems. The important class of conjugated carbanions is amenable to experimental study because such carbanions are relatively stable and are observable both as free anions and as ion pairs in solution and in the gas phase. They are also rather large molecular species from the quantum mechanical standpoint and ab initio calculations for a related series of such systems are presently feasible only with rather limited basis sets. Consequently, our study of such systems required a "calibration" study of simpler carbanions using a variety of basis sets. In this paper we present a study of methyl, ethyl, vinyl, and ethynyl anions using a consistent series of basis sets. No such study of a series of carbanions has yet been published although isolated members of this set have been studied on an individual basis. The most extensively studied of these is methyl anion.[2-7] Several important features have emerged from these studies; for example, with limited basis sets the highest occupied MO of CH_3^- is unbound. This result is known to be due to a truncated basis set[7] and a large basis that includes highly diffuse orbitals is required to bring this orbital down into binding range.[6] Nevertheless, even at the Hartree–Fock limit methyl anion has a higher energy than methyl radical; that is, the electron affinity of methyl radical is less than the correlation energy difference between radical and anion. In effect, in a

Hartree–Fock calculation, methyl anion tends to be methyl radical plus a distant electron subject only to the usual constraint that each MO contains two electrons. Consequently, more limited basis sets may well produce a sufficiently satisfactory description for many purposes. Moreover, since the use of extensive basis sets is not practical for large organic systems, it becomes important to establish how well carbanions can be described with limited bases.

Methyl anion and homologous alkyl anions have not yet been observed in the gas phase.[8,9] They are known in solution only in close association with a metal gegenion in organometallic compounds that have ion pair character and are usually aggregated.

A few simple carbanions are known in the gas phase; the relative proton affinity of ethynyl anion has been established[9] and several measurements of the electron affinity of ethynyl radical have been published.[10-13] An upper limit to the electron affinity of vinyl radical has been reported.[14]

Previous calculations of varying degrees of basis set sophistication have appeared for ethynyl,[15] vinyl,[16,17] and ethyl[17,18] anions.

Calculations

All of the calculations reported in this paper are SCF–LCAO–MO calculations in which no empirical parameters are used. The several basis sets used are described as follows.

STO-NG. The smallest basis set used is the STO-NG basis developed by Hehre, Stewart, and Pople[19] in which a minimum basis consisting of a 1s orbital on hydrogen and 1s, 2s and a set of 2p orbitals on each first row atom are expanded as a linear combination of N Gaussian functions chosen to give a best least-squares fit to the corresponding Slater orbital. The "standard" Slater exponents compiled by the Pople group[18,19] were augmented by values established previously for a carbanion carbon and its attached hydrogens.[5] The exponents used in the present study are summarized in Table I. Geometry and exponent optimizations were carried out using the steepest descent approach at the 3G level with a final calculation for each of the optimized cases and for each reference geometry at the 4G level. Only the STO-4G results are reported here.

SS Basis. In the split shell (SS) basis two functions, an inner and outer part, are used for each atomic orbital. The SS basis is taken from Huzinaga[20] and consists of 8 s and 4 p-type Gaussians on each heavy atom (C, N, O, F) and 4 s-type Gaussians on hydrogen. The Gaussian exponents in these functions, unlike those in the STO-4G basis, were chosen to minimize the energies of the isolated atoms in their ground states. The 8 heavy-atom s functions are grouped into four linear combinations; the first containing the four innermost functions and the second containing the next two functions represent mainly the 1s orbital. The other two groups are valence orbitals and consist of one Gaussian each. Our calculations indicate that this is the way of contracting the 8 s Gaussians into four groups which gives the lowest total energy for the atoms C, N, O, and F. This grouping procedure is consistent with the qualitative rules laid down by Dunning.[21] The p-type and hydrogen s-type functions are each gathered into an inner group of three Gaussians and an outer group consisting of a single Gaussian function. Hydrogen atomic orbitals generally contract in a molecular environment, and to allow for this contraction the hydrogen basis set was scaled by a factor $\eta = 1.15$, optimal for H_2.

Basis Sets with Polarization Functions. The next stage of basis set expansion involves polarization functions, which for our purpose means d-type functions on the heavy atoms and p functions on hydrogen. For acetylene, a d-orbital exponent of 1.0 is optimal and we have used this value in the calculations on acetylene and its derivatives presented below. For the methyl, ethyl, and vinyl species, however, we used a d exponent of 0.8, which we and others[22] have found to be best for methyl anion, and which Pople and coworkers[23] have found to be more generally appropriate for hydrocarbons and carbonium ions. For nitrogen, a d exponent of 0.75, found optimal for ammonia[24] and for oxygen, and a value of 0.9, optimal for water,[25] have been used. An exponent value of 0.9 was chosen for fluorine, based on preliminary calculations on hydrogen fluoride. The SS basis set augmented by d functions is referred to below as the "SS+d" basis. Further improvement via the inclusion of p functions on hydrogen gives the SS+d,p basis. For these calculations, a hydrogen p exponent of 1.0, found to be optimal for the p_σ orbital in H_2, was used. For acetylene, methane, ammonia, and their derivatives, geometry optimizations were carried out at all four levels of basis-set sophistication: STO-4G, SS, SS+d, and SS+d,p. Inclusion of p orbitals on hydrogen did not affect the calculated optimum geometries; hence, no SS+d,p calculations were done for the ethyl or vinyl compounds.

Table I. Slater Exponents Used in STO–NG Calculations

Type C–H	ζ_2(C)[a,b]	ζ_1(H)[b]	Use
C(sp^3)–H	1.75	1.17	CH_4, C_2H_6, CH_3 group of $C_2H_5^-$
C(sp^2)–H	1.697	1.225	C_2H_4, CH_2 group of $C_2H_3^-$
C(sp)–H	1.672	1.31	C_2H_2, CH group of C_2H^-
C^-–H	1.56	1.14	All anionic C and attached H

[a] 1s exponent for all carbon atoms = 5.70. [b] ζ_2(C) = 2s exponent = 2p exponent on carbon; ζ_1(H) = 1s exponent on hydrogen.

Table II. Reference Geometries[a]

Molecule (X_nH_m)	X–X, Å	X–H, Å	∠H–X–H, deg
CH_4		1.085	109.5
C_2H_6	1.531	1.099	107.8
C_2H_4	1.330	1.076	116.6
C_2H_2	1.203	1.061	
NH_3		1.012	106.7
H_2O		0.957	104.5
HF		0.917[b]	

[a] From ref 29 unless otherwise specified. [b] From L. E. Sutton, Ed., *Chem Soc. Spec. Publ.*, No. 18 (1965).

Radicals. Most of the molecules and ions treated here have singlet ground states and computations with each of the basis sets described above were done using the normal Roothaan method for closed shell systems.[26] For the radical species considered below, however, the orthogonality constrained basis-set expansion technique of Hunt and Goddard[27] was used but because of the additional computer time involved in these calculations, they were performed only at the SS+d level.

Geometries. In addition to the equilibrium or minimum energy geometries for the carbanions, it is useful to have a reference molecular geometry defined for each hydrocarbon and derivatives. For this purpose, we found it convenient to use as the reference geometry for each neutral parent molecule the experimentally determined equilibrium geometry. The reference geometry for each anion or radical is that of the parent from which a proton or hydrogen atom, respectively, is removed without other geometric change. Such carbanions are referred to as "subtract" ions.[5] For the vinyl species, a second, "linear", reference geometry is generated from that derived from ethylene by increasing the HCC angle about the anionic or radical carbon to 180°. The reference geometries are summarized in Table II. Many of the calculations were performed for reference geometries because only these geometries are useful for the difference electron density maps to be discussed below.

Table III. Total Energies for Neutral Closed Shell Molecules[a]

Molecule	Energies, au					
	STO–NG	Min STO[c]	STO-4-31G[d]	SS	SS+d	SS+d, p
CH_4	−40.0123	−40.1144	−40.1398	−40.1787	−40.1940	−40.2016
C_2H_2	−76.4123	−76.6185	−76.7111	−76.7922	−76.8199	−76.8252
C_2H_4	−77.6300	−77.8343	−77.9205	−78.0028	−78.0331	...
C_2H_6	−78.8712	−79.0689	−79.1148	−79.1927	−79.2261	...
NH_3	−55.8504[b]	−56.0050	−56.1067	−56.1569	−56.1817	−56.1940
H_2O	−75.4981[b]	−75.6556	−75.9086	−75.9824	−76.0090	−76.0234
HF	−99.2700[b]	−99.4785	−99.8873	−99.9852	−100.0040	−100.0137

[a] In their reference geometries unless otherwise indicated. [b] STO-4G energy using STO-4G optimum exponents and geometry: P. H. Owens, Ph.D. Thesis, Department of Chemistry, University of California, Berkeley, Calif., 1973. [c] Experimental geometries and Slater's rules exponents: W. E. Palke and W. N. Lipscomb, *J. Am. Chem. Soc.*, 88, 2384 (1966) (values for NH_3 and C_2H_2 are the corrected values quoted in ref 19), except for H_2O, which is for a near experimental geometry and Slater's rules exponents (HOH = 105°): R. M. Pitzer and D. P. Merrifield, *J. Chem. Phys.*, 52, 4782 (1970). [d] Energies appropriate to STO-4-31G optimum geometries, from ref 29, except for CH_4, NH_3, H_2O, and HF: from W. A. Lathan, W. J. Hehre, L. A. Curtiss, and J. A. Pople, *J. Am. Chem. Soc.*, 93, 6377 (1971). Slightly different energies are generally given in W. A. Lathan, L. A. Curtiss, W. H. Hehre, J. B. Lisle, and J. A. Pople, *Prog. Phys. Org. Chem.*, 11, 175 (1974).

Table IV. Total Energies of Carbanions, in Their Reference Geometries

Molecule	Energies in au			
	STO-4G	SS	SS+d	SS+d, p
CH_3^-	−39.1878	−39.4559	−39.4712	−39.4777
CH_3^-, planar[a]	−39.1666	−39.4480	−39.4572	−39.4647
C_2H^-	−75.6983	−76.1588	−76.1883	−76.1910
$C_2H_3^-$	−76.8375	−77.3033	−77.3345	
$C_2H_3^-$, linear[b]	−76.7686	−77.2508	−77.2763	
$C_2H_5^-$	−78.0507	−78.4706	−78.5045	

[a] Reference geometry for planar methyl anion has CH = 1.080Å. [b] Vinyl anion with reference geometrical parameters except for *CCH at anionic carbon, which is set = 180°.

Results. In Tables III and IV are summarized the total energies of the systems treated in this paper in their reference geometries. The STO-NG calculations were performed with the modified IBMOL IV program described earlier.[5] The extended basis set calculations were performed using the POLYATOM program.[28]

Table III includes a selection of total energies from other calculations reported in the literature. Of some interest is the comparison between our SS results and those of Pople and coworkers using the split valence-shell STO-4-31G basis.[29] The three basis sets, STO-4G, STO-4-31G, and SS all have the same number of primitive Gaussian functions, but they are grouped differently and with exponents chosen according to different theoretical criteria; of the three, the SS and STO-4-31G give comparable energies and minimum-energy geometries.

Ionization Potentials and Proton Affinities of Carbanions

Two measures of carbanion stability relative to the corresponding radical are given in Table V. One is the approach of Koopmans' theorem in which the ionization potential is approximated as the SCF energy of the highest occupied (lone pair) MO. This MO is bound for ethynyl and vinyl anions but is unbound for methyl and ethyl anions. The latter situation has been discussed by both Duke[6] and the Kutzelnigg[7] group. The incorporation of highly diffuse functions is required to make the energy of the highest occupied MO of methyl anion negative. The amount of electron density far from the nucleus is small;[6] that is, the electron density distribution of methyl anion close to the HF limit differs little from that resulting from the basis sets used in this paper. The ionization potential of CH_3^- (electron affinity of $CH_3\cdot$) given by the SCF energy differences of both species in their standard geometry is −2.04 eV. This value is an approximate vertical ionization potential and may be expected to be more negative than the corresponding adiabatic value for both species in their equilibrium geometries because the methyl radical bending potential is rather shallow. The SCF adiabatic value of the Kutzelnigg group[7] is −1.38 eV, only 0.7 eV higher than our value.

Table V. Ionization Potentials, Proton Affinities, and Bond Dissociation Energies[a]

Anion	(R^-)			
	$C_2H_5^-$	CH_3^-	$C_2H_3^-$	C_2H^-
Ionization Potentials of R^- (eV)				
$-\epsilon_{ho}$[b] SS+d (ref)	−0.53	−0.62	0.54	3.82
$E(R\cdot) - E(R^-)$, SS+d (ref)	−2.13	−2.04	−1.21	1.44
Proton Affinities of R^- (kcal mol^{-1})				
STO-4G (ref)	515	517	497	448
STO-4G (opt)[c]	503	502	479	444
SS (ref)	453	453	439	397
SS+d (ref)	453	453	438	396
SS+d, p (ref)		454		398
Bond Dissociation Energy of R–H (kcal mol^{-1})				
SS+d (ref)	90	93	97	116
Exptl DH°[d]	98	104	108	122

[a] (Ref) and (opt) indicate reference and optimized geometries, respectively. [b] Energy of highest occupied (lone pair) MO. [c] Data from R. A. Wolf, unpublished, and P. H. Owens, Thesis, University of California, Burkeley, Calif., 1973. [d] References 35 and 36.

Table V also lists values of the proton affinities of carbanions given as $E(RH) - E(R^-)$ calculated for the same basis set. For the extended basis sets only the proton affinities for anions in the reference geometries are given since geometry optimization was found to change these proton affinities by only a few kilocalories per mole or less. Polarization functions have about the same effect on carbanion and hydrocarbon and, as shown in Table V, do not much affect the SS computed proton affinities.

The computed proton affinities reflect the expected order of hydrocarbon acidities: $C_2H_2 > C_2H_4 > CH_4 \sim C_2H_6$. Our proton affinity of 396 kcal mol^{-1} for acetylide ion may be compared with other values in the literature,[15] 387 kcal mol^{-1} for a basis set smaller than our SS and 392 kcal mol^{-1} for an unpolarized basis larger than SS. Owens and Streitwieser[5] compute a proton affinity for methyl anion of 442 kcal mol^{-1} with an unpolarized basis larger than SS.

Proton affinities in the Hartree–Fock limit can be estimated for methyl and acetylide anions. For methyl, the energies of the anion found by Duke[6] and of methane found by Clementi and Popkie[30] should be close to the limiting SCF values, and give a proton affinity of 434 kcal mol^{-1}. Similarly, the Hartree–Fock energy for acetylene[31] and a near Hartree–Fock calculation with a large polarized STO basis in acetylide[32] give a proton affinity of 394 kcal mol^{-1}. These Hartree–Fock proton affinities may be expected to be close to the true values since the number of electron pairs does not change and the correlation energy difference is expected to be small.[33] Hopkinson et al.[15a] have shown that a

number of such Hartree-Fock proton affinities correlate well with experimental values. To calibrate our calculations, a similar series is reported in Table VI for the first row anions, F^-, OH^-, NH_2^-, CH_3^-, as well as $C_2H_3^-$ and C_2H^-.

Proton affinities for NH_2^-, OH^-, and F^- are known experimental quantities.[8] We found that there exists an excellent, if empirical, linear relationship between the bond dissociation energies of H_2N-H, HO-H, and H-F and the electron affinities of the corresponding radicals (Figure 1). The corresponding second row hydrides and radicals give a linear correlation of their own with the same slope as the first row hydrides and radicals. The attraction of a radical for an electron appears to be related to its attraction for a hydrogen atom.[8] Extrapolation of this empirical correlation to the DH° of CH_3-H gives an electron affinity for CH_3· of 4 kcal mol^{-1}. This value is close to the 7 kcal mol^{-1} estimated by the Kutzelnigg group[7] with their CI calculations of CH_3^-. Our empirical value is used in Table VI for the calculation of the proton affinity of CH_3^- using the equation

$$PA(R^-) = DH°(R\text{-}H) + IP(H\cdot) - EA(R\cdot)$$

The failure of ethylene to react with hydroxide anion in the gas phase puts an upper limit of ca. 1.3 eV on the electron affinity of vinyl radical.[14] The electron affinity of phenyl radical is between 1.6 and 1.2 eV;[34] assuming that vinyl should have a similar but somewhat smaller electron affinity of ca. 0.9 to 1.3 eV or 25 ± 5 kcal/mol, we get the proton affinity estimate given in Table VI. Several estimates of the electron affinity of acetylide radical have been reported; of these, those from flowing afterglow[9] (2.2 eV) and mass spectrometry (2.1 ± 0.3 eV,[12] 2.2 ± 0.4 eV[13]) give the closest agreement. The values from electron photodetachment (3.73 eV)[11] and from magnetron[10] (2.7 eV) experiments seem to be too high. Values from the magnetron in particular do not seem to be reproducible by other techniques (see, for example, ref 14). Taking the lower values, 50 ± 9 kcal/mol, we get a proton affinity of 386 kcal/mol. Experimental uncertainties in the carbanion proton affinity values just discussed are difficult to estimate but an estimated uncertainty of ±10 kcal mol^{-1} would appear to be reasonable.

Table VI shows that as polarization functions are added to the SS basis the proton affinities relative to fluoride improve, except for acetylide, but the absolute proton affinities are either unchanged (for carbanions) or get worse. This is an indication that to approach more closely the absolute proton affinities we would have to increase the size of the s,p basis on the central atoms C, N, O, F. At the SS+d level, the agreement between experimental and theoretical acidities is good except for acetylide, given the moderate size of the basis and the fact that neither geometries nor d-orbital exponents for the anions are optimal. The relatively low value for the acetylide proton affinity relative to fluoride suggests that a larger value for the electron affinity of acetylide radical (the photodetachment value of 3.73 eV,[11] giving a proton affinity of 350 kcal/mol^{-1}, or −20 relative to fluoride) is more accurate than the 2.2 eV[9,12,13] chosen in making the table.

Table V also compares the present SCF bond dissociation energies calculated as $E(R\cdot) + E(H\cdot) - E(R\text{-}H)$ for the reference structures. In this case we do not expect an absolute comparison with experimental DH° because an electron pair is unpaired in the process with a resultant large change in correlation energy. Nevertheless, the *changes* in bond dissociation energy along the series C_2H_5-H, CH_3-H, C_2H_3-H, and C_2H-H parallel the experimental values[35,36] exactly. The values also parallel the proton affinities of R^- as discussed above for first row systems. In the hydrocarbon

Table VI. Computed and Experimental Proton Affinities[a]

Anion/basis:	SS	SS+d	SS+d,p	Exptl
F^-	394 (0)	406 (0)	412 (0)	370 (0)
OH^-	425 (31)	432 (26)	437 (25)	391 (21)
NH_2^-	447 (52)	449 (43)	451 (39)	407 (37)
CH_3^-	453 (59)	453 (47)	454 (42)	414 (44)
$C_2H_3^-$	439 (45)	438 (32)		397 (27)
C_2H^-	397 (3)	396 (−9)	398 (−14)	386 (16)[b]
				350 (−20)[c]

[a] All values in kcal mol^{-1}; values in parentheses are relative to the proton affinity of fluoride. All species are constrained to their reference geometries. For sources for and derivation of experimental proton affinities, see text. [b] For EA of HC_2· = 2.2 eV. [c] For EA of HC_2· = 3.73 eV.

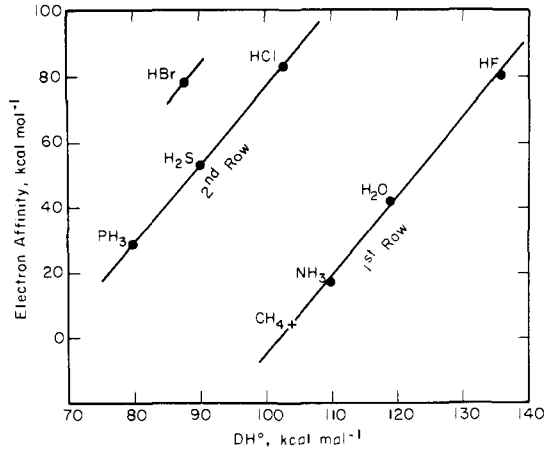

Figure 1. Linear correlations of $\Delta H°$ (Y-H) and EA (Y·). Data taken from ref 8, 35, and 36.

radicals we can argue that the greater the s character in the carbon orbital forming the C-H bond the shorter and stronger the bond and the more s character available for the corresponding carbanion lone pair.

The Electronic Structure of Carbanions

In this section we use the results of the ab initio calculations to discuss the electronic structures of carbanions and the changes in charge distribution that occur when a proton is removed from a hydrocarbon. Our discussion centers mainly on the deprotonation of ethylene (I → II) to give

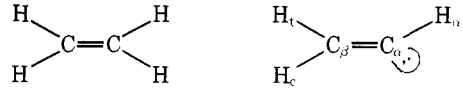

I II

vinyl anion because in this example we can examine changes in both σ and π electronic systems, and in addition, we have a pair of stereochemically distinct β hydrogens. In order not to confuse changes in geometry with changes in electronic reorganization during deprotonation, the reference geometries described above have been used throughout; that is, vinyl anion is derived by removing a proton from ethylene with no other geometric changes.

Gross features of charge distribution can be inferred from some expectation values, such as the dipole moments of a series of related systems. More detailed aspects of electronic structures have commonly been presented in terms of Mulliken population analyses.[37] Such analyses have important limitations, and alternatively, less simple schemes have been proposed.[38,39] Put simply, analyzing molecular populations by partitioning electrons among the constituent atoms and their atomic orbitals is inherently limited by "the fact that a molecule is something new and different from an

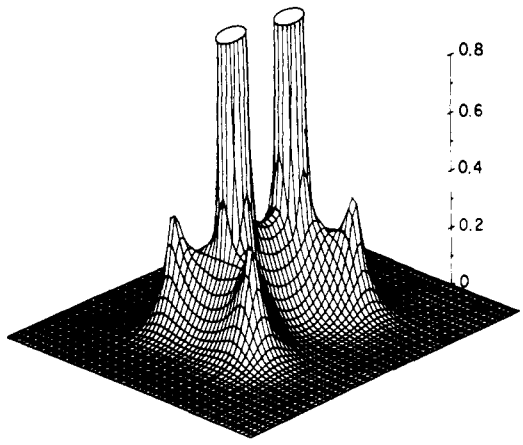

Figure 2. Perspective plot of electron density of ethylene for the molecular plane. The vertical axis gives the electron density in units of e au^{-3} (SS+d basis).

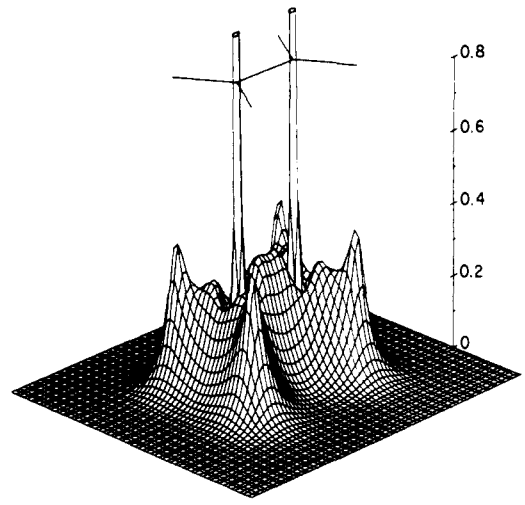

Figure 3. Valence electron density (core electrons deleted) of ethylene for the molecular plane (SS+d basis).

additive combination of atoms".[40] Population analyses are sensitive to the basis set used;[40] for example, electrons close to one atom will be assigned in part to a diffuse orbital centered on another atom. Furthermore, in assigning a single number to the electron population of a given atom, no recognition is given to the possible anisotropic polarization of electrons about the nucleus. Consequently, in the following discussions we have chosen instead to plot electron density functions directly from the computed wave functions. The result gives a clear pictorial representation of the electronic structure of a molecule which readily lends itself to an examination of qualitative patterns of change. Electron density functions have been used frequently in the past in the study of the electronic character of molecules and bonds.[41,42]

Electron Density Functions. Ethylene and Acetylene. The method is exemplified in Figure 2 in which is presented a three-dimensional perspective plot of the total electron density in the molecular plane of ethylene computed with the SS+d basis. At any point in the molecular plane, defined by the four edges of the grid plane, the electron density at each point is measured by the height of the plot above that point in units of electrons au^{-3}. Two obvious features in this plot are the large peaks near the center which indicate the regions of high electron density around the two carbon nuclei, due primarily to the carbon 1s cores. These core peaks so dominate the plot that other features of the electronic structure are obscured. For example, one of the four sharp peaks representing the densities at the four hydrogens is completely blocked out by one of the carbon core peaks. One solution to this problem is a plot of a logarithm function of the electron density which effectively scales up smaller features relative to larger ones.[5,43] The logarithm function has important uses but does suffer the disadvantage of distortion of the electron densities. In order to facilitate comparison with other plots we have chosen here to plot electron density functions directly rather than their logarithms. An alternative solution is shown in Figure 3 in which is plotted only the valence electron density for ethylene. In this plot the core electron densities associated with the 1σ and 2σ molecular orbitals are deleted. All four hydrogen peaks are clearly visible in Figure 2 as is the characteristic "shape" of the in-plane CH bond density, a sharp peak at hydrogen (maximum = 0.42 e au^{-3}) falling rapidly to a ridge (minimum value = 0.29 e au^{-3}), then rising slightly at the carbon valence region before falling to a low valley close to the carbon nucleus. At each carbon nucleus the sharp spike results from the contribution of the 1s-like functions to the valence orbitals required to preserve orthogonality between the valence and core molecular orbitals; alternatively, these spikes may be considered to form the inner part of hydrogenic 2s orbitals centered on carbon.[43] The valley around each carbon results from the spherical node of the hydrogenic 2s orbital but this valley is not a perfect circle because of the admixture of 2p σ AO's and the trigonal asymmetry of the molecular environment. The C–C σ bond is clearly apparent in Figure 3 as a high ridge between the carbon nuclei. Another view of the σ bond is obtained by plotting the σ valence density in the plane of the carbons perpendicular to the molecular plane (the "π plane") as shown in Figure 4. In this figure the bonding ridge of electron density between the carbons stands out clearly. Figure 5 shows a plot of the π MO density in the π plane. The π nodal surface is clearly apparent and, indeed, the overall figure is closely similar to a similar figure derived from a minimum basis set calculation and published previously.[43] In the σ bonds described above the greater charge density at the ends of the bonds, near the nuclei, than at the bond centers is distinctly visible in Figures 3 and 4 although the difference is small. This feature is exaggerated in the π bonds; π overlap is much less efficient than is σ overlap. Figure 5 is plotted on the same scale as the earlier figures. The magnitude of the π electron density is lower than that of the σ density and, in particular, the magnitude at the saddle minimum that corresponds to π bonding is smaller than the corresponding σ electron densities.

These relationships between electron *densities* are undoubtedly real enough but they are also deceptive and emphasize one significant limitation in the use of electron density functions in the interpretation of electronic structure. The total volume associated with the π bond may be greater than that for the σ bond; hence, the electron density functions in Figures 4 and 5 alone do not suffice to tell us the actual numbers of electrons involved in both types of bonding. We are presently exploring the use of other types of functions to minimize these limitations.[44]

Nevertheless, the electron density distributions can provide important understanding of electronic effects.[41] One especially useful aspect of the three-dimensional perspective diagrams is application to various difference electron density functions.[45] One application, for example, makes visible the effect of improvement of basis set. In Figure 6, we plot the difference between the electron density functions calculated for ethylene with the SS+d basis minus that for the STO-4G basis. The extended basis set draws electron density more tightly into the CC bond and provides a better description at the C nuclei. The small changes around hydro-

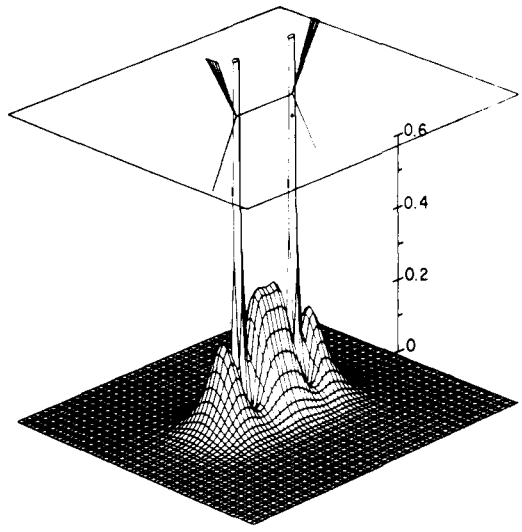

Figure 4. σ valence electron density for the π plane of ethylene (perpendicular to the molecular plane) (SS+d basis).

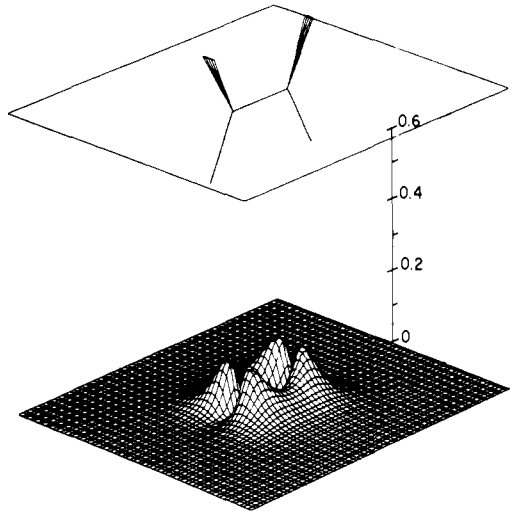

Figure 5. π molecular orbital electron density for the π plane of ethylene (SS+d basis).

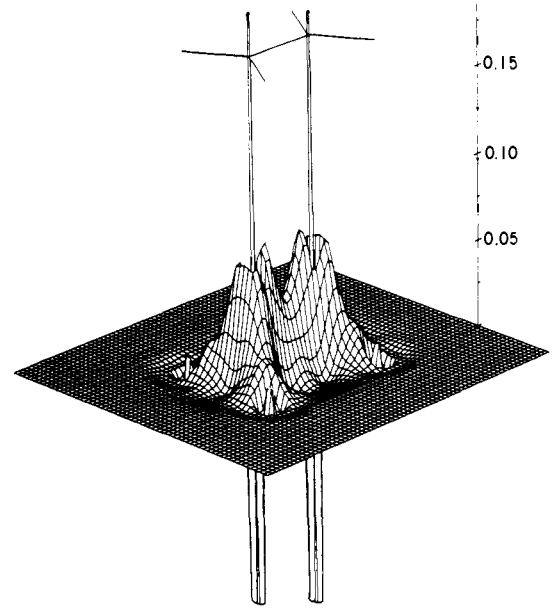

Figure 6. Difference electron density plot for molecular plane of ethylene, ρ(SS+d) − ρ(STO-4G), to show effect of basis set.

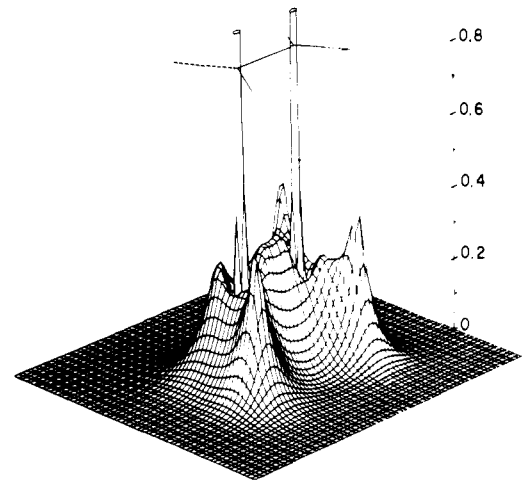

Figure 7. Valence electron density for the molecular plane of vinyl anion in the reference geometry (SS+d basis).

gen show that even minimum basis sets provide an adequate description in these regions. It should be noted that the changes are all rather small; the scale of Figure 6 is multiplied by about fivefold over that in the earlier figures. The effect of extended basis sets in drawing electron density into bonding regions of covalent molecules has been noted before.[42,46]

Vinyl Anion. In Figure 7 is plotted the valence electron density in the molecular plane of vinyl anion as obtained by the SS+d calculation. The dotted line in the superposed figures shows the former location of the proton removed. With the loss of the attractive potential of the proton during deprotonation, the electrons in the associated CH bond fall back toward the nearest positive center, the α-carbon nucleus, as shown in this figure. The resulting lone pair appears as a peak in the ridge of valence density around the α carbon, a peak that is higher and more spread out laterally than the peaks at the carbon end of a normal CH or CC bond. The immediate consequence of deprotonation is to increase greatly the number of electrons in the valence region immediately around the α carbon; to alleviate electron repulsions, we find that electron density in bonds to the α carbon is polarized away, toward the β carbon and α hydrogen, with transfer of σ density to these atoms. Note that the ridge corresponding to the in-plane CC bond density is higher at the β-carbon end, indicative of such bond polarization. From Figure 7 we might conclude that a straight- by which the anionic lone pair is accommodated by the rest of the molecule.

In Figure 8 is shown the π electron density of vinyl anion. The qualitative result is as expected; electron density is transferred from the more electropositive α carbon of the carbanion to the β carbon.

To examine these electronic changes in a more detailed way, we show in Figure 9 a plot of the difference electron density between vinyl anion and ethylene in the molecular plane. The difference is plotted so that positive peaks denote regions where density is greater in the anion than in ethylene; that is, the plot shows the changes in electron density that accompany the removal of the proton. The plot scale is expanded by a factor of 4.5 relative to that of the earlier valence density plots in order to show up the differences more distinctly. Ethylene and vinyl anion are isoelectronic; hence, the electron density difference function must integrate to zero over all space. However, since only a single plane is represented in Figure 9 the difference function need not sum to zero within any given plane, particularly since the inclusion of carbon d-type polarization functions provides

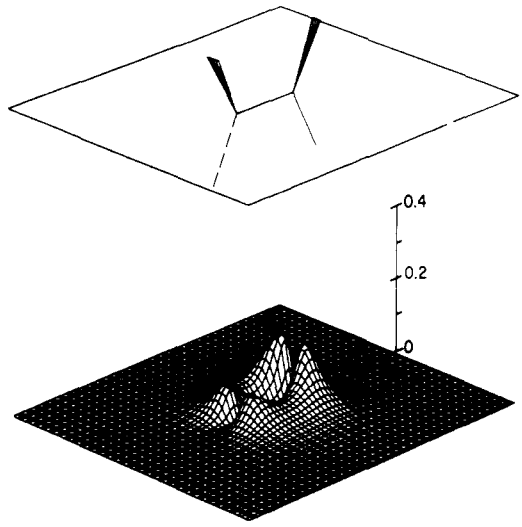

Figure 8. π electron density for vinyl anion (SS+d basis).

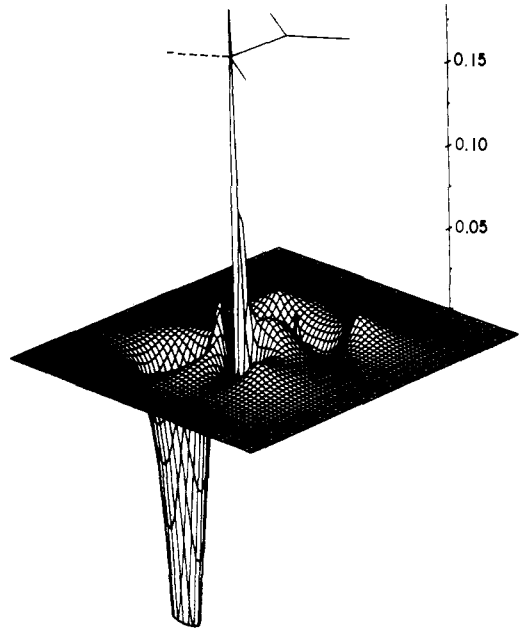

Figure 9. Difference electron density plot showing the effect of removing a proton from ethylene keeping other nuclear positions unchanged, $\rho(C_2H_3^-) - \rho(C_2H_4)$ (SS+d basis), for the molecular plane.

sufficient flexibility to spread the σ MO's out of the molecular plane.

The largest single feature in Figure 9 is the massive well centered on the position of the proton removed to form the anion and demonstrates that the electron density associated with this proton and its CH bond has moved away from this region. These formerly CH bonding electrons have clearly shifted into the lone pair and especially into the lone pair back-lobe regions, onto the α and β hydrogens, and onto the α carbon, right at the nucleus. The large magnitude of this depression relative to the rest of the plot makes it appear that there has been a net loss of electrons in the molecular plane. This is not true, for there are large regions to the sides of the lone pair peak and out beyond the CH bonds where the increased density shows up in Figure 9 only as a slight swelling from the reference plane and does not appear even in the contour plot of the density difference function in Figure 10. A logarithm plot of the difference function, not included here, shows up these small features more clearly. The total volume associated with the small features is much larger than that of the CH bond and emphasizes again the

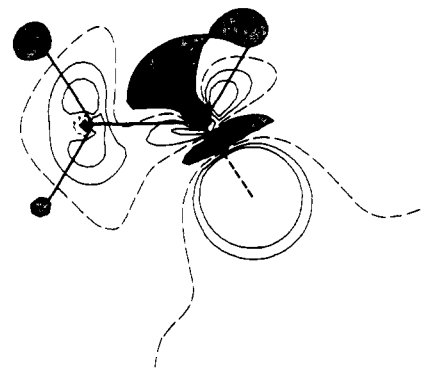

Figure 10. Contour plot corresponding to Figure 9 (SS+d basis).

difference between electron density and numbers of electrons.

The gains in electron density in the lone pair region and at the hydrogens are in agreement with a simple inductive model for the carbanion. However, Figure 9 shows that there are regions in the molecule that have lost electron density. The α-CH bond, for example, has lost electron density although density has increased near the α-hydrogen nucleus. Changes in the CC bond are rather small but the β carbon and the β-CH bonds have lost electron density except close to the atomic nuclei. Both diagrams in Figures 9 and 10 show the effects of charge alternation, rather than an inductive effect, as has been suggested before in connection with other systems.[47] These effects can be understood in terms of waves of polarization; that is, a molecule in which a carbanion lone pair is generated reaches its greatest stability not through a uniform inductive electron transfer and charge dispersal but by creation of regions of high and low electron density *relative to the neutral parent.* The lone pair charge displaces electron density away from immediately adjacent regions to regions just beyond; each of these electron density increases in turn causes displacement away from its immediately adjacent regions to other regions still further beyond.

How real are these electron density difference plots and how valid is the conclusion that polarization is the principal mechanism by which the carbanion negative charge is stabilized in vinyl anion? We submit that the qualitative picture is probably correct. A similar difference plot using a minimum basis set shows the same general features with differences only of relative magnitude. The recent extensive calculations on methyl anion[6,7] suggest that diffuse orbitals are necessary to approach the HF limit for most carbanions; however, the addition of such functions to the basis set would produce electron density changes in the nether regions barely perceptible on the scale of our plots. The small effect of extended basis sets on proton affinities of carbanions is in keeping with this result. Going beyond Hartree–Fock with consideration of electron correlation introduces further uncertainty. Hartree–Fock electron density distributions are known to be correct to second order but this generalization does not, of course, apply to electron density *difference* functions. Nevertheless, the constancy of pair correlations in ionization of C–H bonds suggests that the true time average electron density distribution is little different from the HF distribution.

Another perspective on the changes in electron structure attendant on deprotonation of ethylene is found by examination of the π plane. The difference electron density plot shown in Figure 11 shows the kind of charge displacement anticipated from the asymmetric π density of vinyl anion seen in Figure 8. Electron density is largely transferred from the α carbon to the β; the bifurcated nature of these

Table VII. Mulliken Populations of Ethylene and Vinyl Anion[a]

	C_α			C_β					
	σ	π	Total	σ	π	Total	H_α	H_t	H_c
Atomic Populations									
$C_2H_3^-$	5.82 (5.91)	0.68 (0.76)	6.50 (6.68)	5.25 (4.98)	1.32 (1.24)	6.57 (6.22)	1.01 (1.04)	0.98 (1.04)	0.94 (1.02)
C_2H_4	5.40 (5.16)	1.00 (1.00)	6.40 (6.16)	5.40 (5.16)	1.00 (1.00)	6.40 (6.16)	0.80 (0.92)	0.80 (0.92)	0.80 (0.92)
Δ	0.419 (0.751)	−0.32 (−0.236)	0.098 (0.515)	−0.154 (−0.184)	0.321 (0.236)	0.167 (0.052)	0.213 (0.126)	0.179 (0.124)	0.145 (0.103)

	CC								
	σ	π	Total	CH_α	CH_t	CH_c			
Overlap Populations									
$C_2H_3^-$	1.00 (0.79)	0.53 (0.41)	1.53 (1.21)	0.62 (0.682)	0.76 (0.77)	0.70 (0.80)			
C_2H_4	0.70 (0.82)	0.55 (0.40)	1.25 (1.22)	0.80 (0.79)	0.80 (0.79)	0.80 (0.79)			
Δ	0.308 (−0.030)	−0.024 (0.016)	0.284 (−0.014)	−0.180 (−0.116)	−0.036 (−0.022)	−0.098 (0.004)			

[a] Results given as SS+d basis (STO-4G basis).

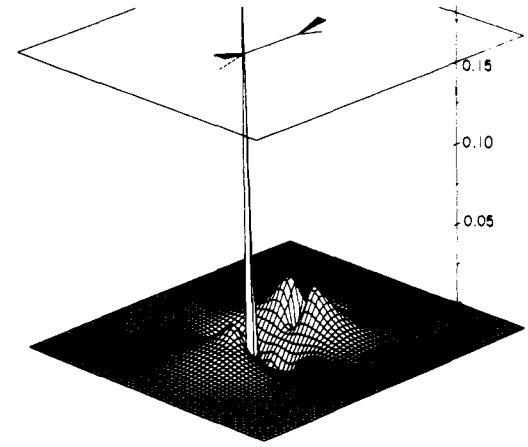

Figure 11. Deprotonation of ethylene: difference electron density plot for π plane (SS+d basis).

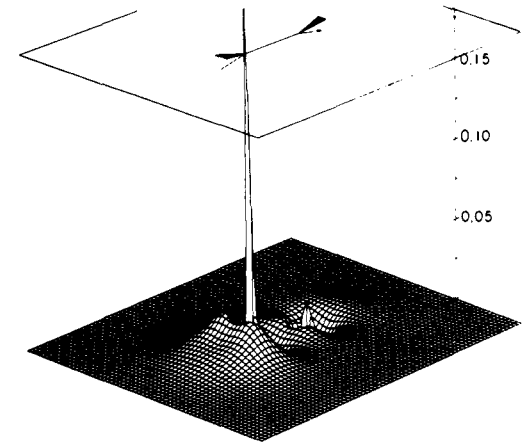

Figure 12. Deprotonation of ethylene: difference density plot for σ electrons in the π plane (SS+d basis).

changes suggests the role of π electrons. However, inspection of the σ-electron changes only for the π plane in Figure 12 is additionally revealing. We see the loss of electron density in the C–C bond close to C_α and in the immediate vicinity of C_β. However, except for the regions close to the carbon nuclei, the two major regions of gain are bifurcated. The overall pattern is again interpretable on the basis of polarization. The creation of the vinyl anion lone pair results in polarization of σ electrons on either side of the molecular plane near the lone pair. The additional polarization of π density to the β carbon results in polarization away of σ electrons from the π region.

An important question at this point concerns the extent to which the Mulliken populations summarized in Table VII reflect these electron density shifts. The atomic population differences from both the SS+d and the STO-4G calculations do generally reflect the changes noted in Figure 9: that is, an increase in σ population at C_α and a decrease in C_β, vice versa for the π electrons, and an increase in the electron population of the hydrogens, the gain being larger at the hydrogen trans to the lone pair than at the cis hydrogen. Similarly, the decreases in CH overlap populations are consistent with the losses of CH bond densities in the difference plots although the magnitudes of the losses in the β-CH bonds appear to be too small. The CC overlap populations, especially as given by the SS+d basis, are not in accord with Figure 9. Most of the gross features of the difference plots are qualitatively reproduced by the population analyses but the quantitative features are not; furthermore,

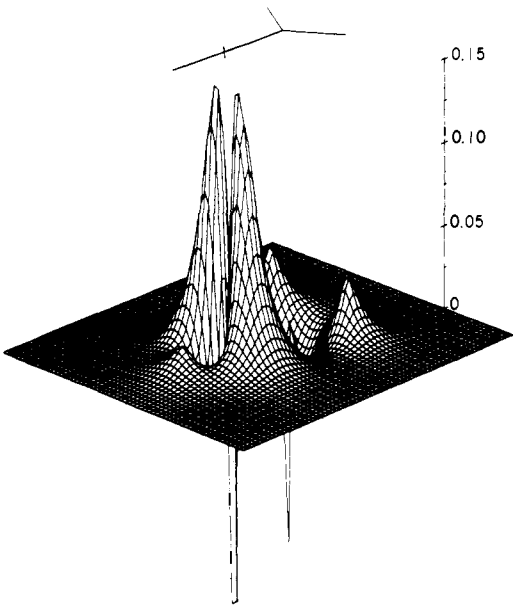

Figure 13. Electron density difference plot for ionization of linear vinyl radical, $\rho(C_2H_3\cdot) - \rho(C_2H_3^+)$ (SS+d basis).

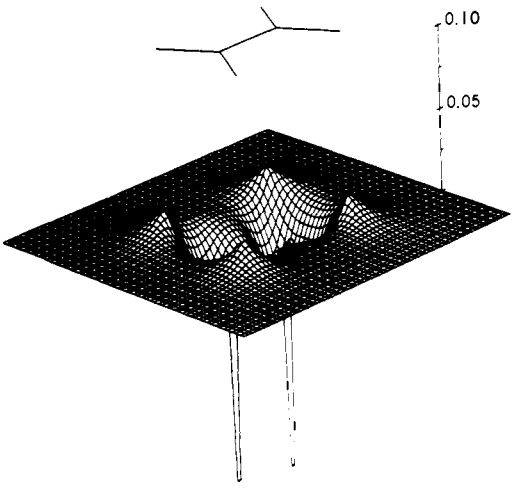

Figure 14. Electron density difference plot for ionization of ethylene, $\rho(C_2H_4) - \rho(C_2H_4^+)$ (SS+d basis).

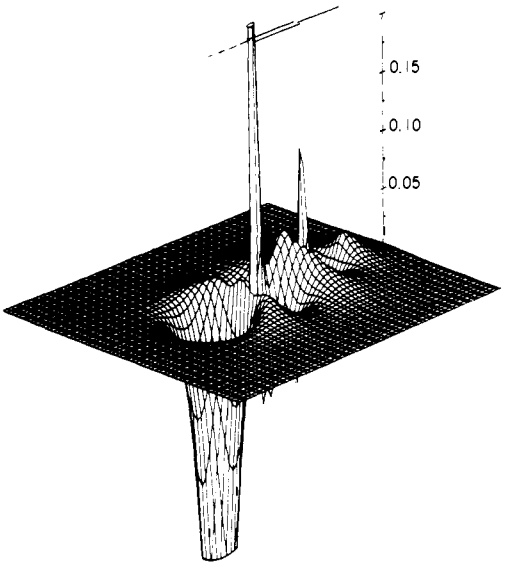

Figure 15. Electron density difference plot for deprotonation of acetylene, $\rho(C_2H^-) - \rho(C_2H_2)$ (SS+d,p basis).

the anisotropy of the polarization effects shown by the difference plots do not show up in the population analyses.

The polarization wave pattern of peaks and valleys shown in Figures 9 and 10 for vinyl anion–ethylene are typical of other systems as well. One might expect that formation of a carbanion by deprotonating a hydrocarbon would be similar to adding an electron to a neutral radical. Indeed, a plot of the electron density difference, vinyl anion minus vinyl radical (not reproduced here), is almost identical with Figure 9 except for the absence of the large depression associated with the C–H bonding electrons. The corollary that the electron density distributions of ethylene and vinyl radical are similar is not surprising. In fact, many of the features of Figure 9 are preserved even in the absence of anionic charge or lone pairs. As an example, Figure 13 displays the electron density difference plot, $\rho(\text{linear } CH_2{=}CH\cdot) - \rho(CH_2{=}CH^+)$. The "extra" electron causes a large bifurcated peak, largely 2p orbital in character, but is also distributed to the three hydrogens. As before, there is loss of electron density in the α-CH and CC bond regions and around the β carbon.

In contrast, a wholly different pattern results from removing a π electron from ethylene to form ethylene radical cation. The corresponding difference plot for the molecular plane, Figure 14, shows the effects of reducing σ–π repulsions by removal of a π electron. σ density moves in from the hydrogens toward the carbons and the CC bond region. Precisely the opposite process occurs on addition of an electron to ethylene to form the radical anion.

Deprotonation of acetylene gives an electron density difference plot, Figure 15, that shows many of the same features as deprotonation of ethylene. The increase in electron density in the back lobe of the acetylide lone pair puts additional density in the CC bond region. The depletion of CH bond density and the polarization of π electrons are exactly as discussed above for ethylene and vinyl anion. Ethane shows comparable electron density changes on deprotonation despite the absence of readily polarizable π electrons. The pattern of density shifts in the plane of the lone pair and its antihydrogen are much the same as those for vinyl anion in Figure 9.[54] Indeed, since the effects of deprotonation on the σ systems of acetylene, ethylene, and ethane are so similar, the relative hydrocarbon acidities may be due as much to the polarizability of π electrons as to the amount of s character in the carbanion lone pair.

Molecular Geometry of Carbanions

To construct Figure 9, vinyl anion was constrained to the same geometry as ethylene; the electron density changes in this figure suggest the structural changes that will occur in vinyl anion to reach its minimum energy. Losses of CH and CC bond densities suggest that these bond distances will increase. Indeed, the loss of α-CH density and the increase in density at the α hydrogen suggest the possibility of α elimination for a more electronegative substituent; that is, these electron density changes can be related to organic chemistry. Similarly, the greater increase in density at the hydrogen trans to the lone pair compared to cis suggests a normal trans E2 elimination. If we assume that bond angles will change so as to move internuclear regions out away from charge depletion, then the bond angle around the α carbon should decrease. These generalizations are indeed borne out by the minimum energy geometries summarized in Table VIII. Total energies of the optimized structures are given in Table IX and compared with available literature values.

Table VIII. Optimized Molecular Geometries[a]

Species	Basis	CH	HCH	Species	Basis	NH	HNH
CH_3^-	4G[b]	1.189	97.5	NH_3	4G	1.029	104.3
	SS	1.105	107.3		SS	1.008	113.9
	SS + d	1.101	104.4		SS + d	1.006	106.3
	SS + d,p	1.102	104.2		SS + d,p	1.006	106.6
	Ref 7	1.095	110.4		Ref 24	1.00	107.2
					(Exptl)	1.012	106.7
CH_3^-, planar	4G[b]	1.130	(120)	NH_3, planar	4G[c]	1.010	(120)
	SS	1.082	(120)		SS	0.988	(120)
	SS + d	1.079	(120)		SS + d	0.990	(120)
	SS + d,p	1.080	(120)		SS + d,p	0.987	(120)
	Ref 7	1.075	(120)		Ref 24	0.984	(120)
CH_4	4G[b]	1.089	109.5	NH_4^+	4G[c]	0.724	109.5
	SS	1.084	109.5		SS	1.017	109.5
	SS + d	1.082	109.5		SS + d	1.019	109.5
	SS + d,p	1.084	109.5		SS + d,p	1.016	109.5
	(Exptl)	1.085	109.5				

		CH	CC	Species	Basis	CH	CC
C_2H_2	4G[c]	1.063	1.187	C_2H^-	4G	1.062	1.213
	SS	1.050	1.192		SS	1.056	1.240
	SS + d	1.056	1.182		SS + d	1.060	1.229
	SS + d,p	1.058	1.182		SS + d,p	1.061	1.229
	(Exptl)	1.061	1.203				

		CC	α-CH	$CC_\alpha H$	$HC_\beta H$	CH_c	CH_t	CCH_t
$C_2H_3^-$	4G[c]	1.356	1.198	107.4	104.8	1.128	1.154	130.7
	SS	1.367	1.114	110.6	111.7	(1.076)	(1.076)	(124.2)[d]
	SS + d	1.351	1.110	108.0	111.7	(1.076)	(1.076)	(124.2)[d]
$C_2H_3^-$, linear	4G[c]	1.335	1.184	(180)	105.2	1.148	1.148	
	SS	1.321	1.054	(180)	109.2	(1.076)	(1.076)	
	SS + d	1.310	1.055	(180)	108.7	(1.076)	(1.076)	

[a] Bond lengths in Å, bond angles in degrees; experimental results as quoted in Table III. [b] Reference 5. [c] R. A. Wolf, unpublished results. [d] Local C_{2v} symmetry about C_β assumed, CH_β lengths not optimized.

Table IX. Energies of Species in Optimum Geometries[a]

Species	STO-4G	SS	SS + d	SS + d,p	Lit.
CH_4	−40.0121[b]	−40.1787	−40.1940	−40.2016	−20.2136[c]
CH_3^-	−39.2123[b]	−39.4572	−39.4741	−39.4805	−39.5222[d]
CH_3^-, planar	−39.1719[b]	−39.4480	−39.4572	−39.4647	−39.5195[d]
CH_3^-, ΔE(inv)	25.2[b]	5.8	10.6	9.9	1.7[d]
NH_4^+[e]	−56.2828[f]	−56.5123	−56.5297	−56.5463	
NH_3[e]	−55.8504[f]	−56.1598	−56.1817	−56.1940	−56.2219[g]
NH_3, planar[e]	−55.8338[f]	−56.1593	−56.1701	−56.1845	−56.2138[g]
NH_3, ΔE(inv)	10.4	0.3	7.3	6.0	5.1[g]
C_2H_2	−76.4130[f]	−76.7925	−76.8208	−76.8260	−76.8540[h]
C_2H^-	−75.7060[f]	−76.1613	−76.1894	−76.1921	−76.2151[i]
E (PA)	0.7070	0.6312	0.6314	0.6339	0.6383
$C_2H_3^-$	−76.8677	−77.3098	−77.3345		−77.3198[j]
$C_2H_3^-$, linear	−76.7846[f]	−77.2529	−77.2788		−77.2519[j]
$C_2H_3^-$, ΔE(inv)	52.1	35.7	35.0		38.9[j]

[a] Total energies in au, inversion barriers in kcal mol^{-1}. [b] Reference 5. [c] Reference 30. [d] Reference 6. [e] Energies for NH_4^+ and NH_3 in SS, SS + d, and SS + d,p basis sets are interpolated from geometry optimization studies; calculations at the final optimized geometries were not made. [f] R. A. Wolf, unpublished results. [g] References 24 and 49. [h] Reference 31. [i] Reference 32. [j] Reference 16. These calculations use more s and p basis functions than our SS basis, but no d functions.

Comparing the results for the several basis sets in Table VIII leads to some generalizations. The lengthening of bonds and contraction of bond angles is exaggerated by the STO-4G basis. This tendency has been noted previously.[5,48] Like the similar STO-4-31G basis,[48] the SS calculations give shorter bonds and bond angles which are, in general, too large. This defect is removed by addition of polarization functions. For ammonia in particular, these generalizations are well documented.[24,49]

The situation with respect to methyl anion, however, is particularly confused. Our medium sized basis sets indicate bond angles that are smaller and an inversion barrier that is larger than for ammonia (Tables VII and IX). A similar result was found by Lehn and coworkers[16] comparing vinyl anion with methylenimine. The SS+d,p basis gives an ammonia barrier close to the experimental value. However, the recent calculations on methyl anion incorporating highly diffuse p orbitals on carbon present a different story.[6,7] As discussed above with reference to electron affinities the problem with methyl anion could well be its Hartree–Fock instability relative to methyl radical and an electron. Thus, the use of highly diffuse orbitals leads to wider HCH bond angles and a low inversion barrier, less than half that of ammonia.[6,7] It is noteworthy in this connection that unrestricted Hartree–Fock STO 4-31G calculations predict that a singlet diradical configuration of methyl anion, approximately methyl radical plus a loosely bound electron in a diffuse MO of lone-pair symmetry, is more stable than the

normal closed shell singlet configuration.[50] Consequently, the computed structure and inversion barrier of methyl anion as calculated by HF methods are relatively unreliable and do not serve as a realistic reference for other systems.

The only experimental information available concerning the inversion barrier of methyl anion comes from an infrared study of Andrews[51] of matrix-isolated methyllithium monomer. Andrews found a linear correlation between the symmetric HCH deformation frequencies of a series of singly substituted methanes and substituent electronegativity. The value found for methyllithium lies on the correlation line and permits extrapolation to a substituent electronegativity of zero; that is, methyl anion. His predicted frequency of 970 cm^{-1} is 20 cm^{-1} higher than ammonia and suggests that the inversion barrier for methyl anion should be greater than that of ammonia. Methyl anion may well be unique among carbanions for quantum mechanical study. Ethyl anion is probably also less stable than ethyl radical in the Hartree–Fock limit but the effects of the added charge may well be muted by the polarizable methyl substituent. Vinyl and acetylide anions have bound highest occupied MO's even with moderate basis sets and their calculated geometries should be more reliable.

A further consideration that makes methyl anion a uniquely different system to study by LCAO methods concerns symmetry. In the case of ammonia, it is well-documented that polarization functions must be applied with care to the calculation of the inversion barrier because two of the nitrogen d functions cannot by symmetry contribute to the wave function of planar ammonia but can contribute to the pyramidal structure.[52] These considerations apply equally to methyl anion. As a result, the effects of d orbitals on bond angles and inversion barriers are much greater in NH_3 and CH_3^- than, for example, in vinyl anion, for which these symmetry arguments do not apply.

The inversion barrier of vinyl anion has been estimated as 25–35 kcal mol^{-1} based on experimental kinetic data for dehydrobromination of 1,2-dibromoethylenes in methanolic methoxide.[53] The relevance of this estimate to our calculations, which apply to the isolated, nonhydrogen-bonded species in the dilute gas phase, is open to question. Our computed barrier for vinyl anion, 34 kcal mol^{-1} (Table IX), is in good agreement with this experimental estimate and with the value calculated by Lehn, Munsch, and Millie, 39 kcal mol^{-1}.[16] The alternative mechanism for inversion involving twisting about the CC bond through a nonplanar transition state was found by Lehn et al.[16] to be much higher in energy for methylenimine than in-plane inversion. Consequently, the out-of-plane inversion process for vinyl anion was not given additional consideration, although it may, in fact, be a reasonable pathway for a hydrogen-bonded vinyl anion.

Acknowledgment. We gratefully acknowledge the use of Professor H. F. Schaefer's versions of the POLYATOM and atomic programs, and Dr. W. H. Hunt's OCBSE program. We thank Professor Schaefer, Dr. Hunt, and Mr. P. Pearson for discussions concerning the use of these programs and for helpful comments regarding this work.

References and Notes

(1) Supported in part by NSF Grant No. GP-29383 and USPH Grant No. GM-12855. Additional computer time was donated by the Computer Center, University of California.
(2) Earlier calculations are reviewed in L. Radom and J. A. Pople, *Org. Chem., Ser. One*, 71 (1972), and in W. G. Richards, T. E. H. Walker, and R. K. Hinkley, "A Bibliography of ab initio Molecular Wave Functions", Oxford University Press, London, 1971.
(3) R. E. Kari and I. G. Csizmadia, *J. Chem. Phys.*, **56**, 4337 (1972).
(4) R. E. Kari and I. G. Csizmadia, *Int. J. Quantum Chem.*, **6**, 401 (1972).
(5) P. H. Owens and A. Streitwieser, Jr., *Tetrahedron*, **27**, 4471 (1971).
(6) A. J. Duke, *Chem. Phys. Lett.*, **21**, 275 (1973).
(7) F. Driessler, R. Ahlrichs, V. Staemmler, and W. Kutzelnigg, *Theor. Chim. Acta*, **30**, 315 (1973); see also R. Ahlrichs, F. Driessler, H. Lischka, and V. Staemmler, *J. Chem. Phys.*, **62**, 1235 (1975).
(8) J. I. Brauman, J. R. Eyler, L. K. Blair, M. J. White, M. B. Comisarow, and K. C. Smyth, *J. Am. Chem. Soc.*, **93**, 6360 (1971).
(9) D. R. Bohme, E. Lee-Ruff, and L. B. Young, *J. Am. Chem. Soc.*, **94**, 5153 (1972).
(10) F. M. Page and G. C. Goode, "Negative Ions and the Magnetron", Wiley-Interscience, New York, N.Y., 1969.
(11) D. Feldmann, *Z. Naturforsch., Teil A*, **25**, 621 (1970).
(12) R. Locht and J. Momigny, *Chem. Phys. Lett.*, **6**, 273 (1970).
(13) B. M. Hughes, C. Lifshitz, and T. O. Tiermann, *J. Chem. Phys.*, **59**, 3162 (1973).
(14) D. K. Bohme and L. B. Young, *J. Am. Chem. Soc.*, **92**, 3301 (1970).
(15) (a) A. C. Hopkinson, N. K. Holbrook, K. Yates, and I. G. Csizmadia, *J. Chem. Phys.*, **49**, 3896 (1968); (b) A. C. Hopkinson and I. G. Csizmadia, *J. Chem. Soc. D*, 1291 (1971).
(16) J. M. Lehn, B. Munsch, and P. Millie, *Theor. Chim. Acta*, **16**, 351 (1970).
(17) A. Streitwieser, Jr., P. H. Owens, R. A. Wolf, and J. E. Williams, Jr., *J. Am. Chem. Soc.*, **96**, 5448 (1974).
(18) P. H. Owens, R. A. Wolf, and A. Streitwieser, Jr., *Tetrahedron Lett.*, 3385 (1970).
(19) W. H. Hehre, R. F. Stewart, and J. A. Pople, *J. Chem. Phys.*, **51**, 2657 (1969); J. A. Pople, *Acc. Chem. Res.*, **3**, 217 (1970).
(20) S. Huzinaga, *J. Chem. Phys.*, **42**, 1293 (1965); S. Huzinaga, D. McWilliams, and B. Domsky, *ibid.*, **54**, 2283 (1971).
(21) T. J. Dunning, Jr., *J. Chem. Phys.*, **53**, 2823 (1970); *Chem. Phys. Lett.*, **7**, 423 (1970).
(22) R. E. Kari and I. G. Csizmadia, *J. Chem. Phys.*, **46**, 1807, 4585 (1967); **50**, 1443 (1969); M. A. Robb and I. G. Csizmadia, *Int. J. Quantum Chem.*, **5**, 605 (1971).
(23) P. C. Hariharen, W. A. Latham, and J. A. Pople, *Chem. Phys. Lett.*, 14, 385 (1972); P. C. Hariharem and J. A. Pople, *ibid.*, **16**, 217 (1972).
(24) A. Rauk, L. C. Allen, and E. Clementi, *J. Chem. Phys.*, **52**, 4133 (1970).
(25) D. Hankins, J. W. Moskowitz, and F. H. Stillinger, *J. Chem. Phys.*, **53**, 4544 (1970).
(26) C. C. J. Roothaan, *Rev. Mod. Phys.*, **23**, 69 (1951).
(27) W. J. Hunt and W. A. Goddard, *Chem. Phys. Lett.*, **3**, 414 (1969).
(28) I. G. Csizmadia, M. C. Harrison, J. W. Moskowitz, S. Seung, B. T. Sutcliffe, and M. P. Barnett, the POLYATOM System, Technical Notes No. 36 and 40, Cooperative Computing Laboratory, MIT, Quantum Chemistry Program Exchange, Catalog 47A.
(29) R. Ditchfield, W. J. Hehre, and J. A. Pople, *J. Chem. Phys.*, **54**, 724 (1971).
(30) E. Clementi and H. Popkie, *J. Chem. Phys.*, **57**, 4870 (1972).
(31) A. D. McLean and M. Yoshimine, *IBM J. Res. Dev., Suppl. 1*, (Nov. 1967).
(32) J. Gasteiger, unpublished results.
(33) L. C. Snyder, *J. Chem. Phys.*, **46**, 3602 (1967); L. C. Snyder and H. Basch, *J. Am. Chem. Soc.*, **91**, 2189 (1969).
(34) D. K. Bohme and L. B. Young, *Can. J. Chem.*, **49**, 2918 (1971).
(35) D. M. Golden and S. W. Benson, *Chem. Rev.*, **69**, 125 (1969).
(36) S. W. Benson, personal communication.
(37) R. S. Mulliken, *J. Chem. Phys.*, **23**, 1833, 1841, 2338, 2343 (1955).
(38) For example, L. C. Allen, *Annu. Rev. Phys. Chem.*, **20**, 315 (1969).
(39) R. F. W. Bader and P. M. Bedell, *J. Am. Chem. Soc.*, **95**, 305 (1973).
(40) R. S. Mulliken, *J. Chem. Phys.*, **36**, 3428 (1962).
(41) Some examples are M. Roux et al., *J. Chim. Phys. Phys.-Chim. Biol.*, **54**, 218, 939 (1956); **55**, 754 (1958); **57**, 53 (1960); *J. Chem. Phys.*, **37**, 933 (1962); R. M. Pitzer and W. N. Lipscomb, *ibid.*, **39**, 1995 (1963); A. C. Wahl, *Science*, **151**, 961 (1966); D. B. Boyd and W. N. Lipscomb, *J. Chem. Phys.*, **46**, 910 (1967); R. F. W. Bader, W. H. Henneker, and P. E. Cade, *ibid.*, **46**, 3341 (1967); P. E. Cade, R. F. W. Bader, W. H. Henneker, and I. Keaveny, *ibid.*, **50**, 5313 (1969); D. B. Boyd, *ibid.*, **52**, 4846 (1970); T. H. Dunning, Jr., and N. W. Winter, *ibid.*, **55**, 3360 (1971).
(42) C. W. Kern and M. Karplus, *J. Chem. Phys.*, **40**, 1374 (1964); B. J. Ransil and J. J. Sinai, *ibid.*, **46**, 4050 (1967).
(43) A. Streitwieser, Jr., and P. H. Owens, "Orbital and Electron Density Diagrams", Macmillan, New York, N.Y., 1973.
(44) J. M. McKelvey, results to be published.
(45) For example, see A. Streitwieser, Jr., J. E. Williams, J. Cambray, and P. H. Owens, "Proceedings of International Conference on Computers in Chemical Research and Education", Ljubljana, Zagreb, July 12–17, 1973, p 4.
(46) P. R. Smith and J. W. Richardson, *J. Phys. Chem.*, **69**, 3347 (1965); B. D. Boyd, *J. Chem. Phys.*, **52**, 4846 (1970); E. A. Laws, R. M. Stevens, and W. N. Lipscomb, *J. Am. Chem. Soc.*, **94**, 4461 (1972).
(47) W. J. Hehre and J. A. Pople, *J. Am. Chem. Soc.*, **92**, 2191 (1970).
(48) W. A. Latham, W. J. Hehre, L. A. Curtiss, and J. A. Pople, *J. Am. Chem. Soc.*, **93**, 6377 (1971).
(49) R. M. Stevens, *J. Chem. Phys.*, **55**, 1725 (1971).
(50) J. M. McKelvey, unpublished results.
(51) L. Andrews, *J. Chem. Phys.*, **47**, 4834 (1967).
(52) H. F. Schaefer, III, "The Electronic Structure of Atoms and Molecules", Addison-Wesley, Reading, Mass., 1972.
(53) S. I. Miller and W. G. Lee, *J. Am. Chem. Soc.*, **81**, 6313 (1959).
(54) NOTE ADDED IN PROOF: see A. Streitwieser, Jr., and J. E. Williams, Jr., *J. Am. Chem. Soc.*, **97**, 191 (1975).